

Meeting on Ferroelectricity, Zurich, Switzerland, 22-26 September 1975 (to be published).

⁴V. M. Berezov, Ya. Ya. Asadullin, and V. D. Korepanov, *Zh. Eksp. Teor. Fiz.* **69**, 1674 (1975) [*Sov. Phys. JETP* (to be published)].

⁵P. I. Kuindersma, S. Huizenga, J. Kommandeur, and G. A. Sawatzky, *Phys. Rev. B* **13**, 496 (1976).

⁶R. L. Melcher and N. S. Shiren, *Phys. Rev. Lett.* **36**, 888 (1976).

⁷K. Kajimura, K. Fossheim, R. L. Melcher, and N. S. Shiren, *Bull. Am. Phys. Soc.* **21**, 293 (1976).

⁸R. W. Gould, *Phys. Lett.* **19**, 477 (1965).

⁹G. F. Herrmann, D. E. Kaplan, and R. M. Hill, *Phys. Rev.* **181**, 829 (1969).

¹⁰B. D. Laikhtman, *Fiz. Tverd. Tela* **17**, 3278 (1975) [*Sov. Phys. Solid State* **17**, 2154 (1976)].

¹¹N. N. Krainik, V. V. Lemanov, S. N. Popov, and G. A. Smolenskii, *Fiz. Tverd. Tela* **17**, 2462 (1975) [*Sov. Phys. Solid State* **17**, 1635 (1976)].

¹²D. E. Kaplan, R. M. Hill, and G. F. Herrmann, *J. Appl. Phys.* **40**, 1164 (1969); G. F. Herrmann, R. M. Hill, and D. E. Kaplan, *Phys. Rev.* **156**, 118 (1967).

Origin of Raman Scattering and Ferroelectricity in Oxidic Perovskites

R. Migoni and H. Bilz

Max-Planck-Institut für Festkörperforschung, 7000 Stuttgart-80, West Germany

and

D. Bäuerle

Fachbereich Physik der Universität Osnabrück, 4500 Osnabrück, West Germany

(Received 9 July 1976)

The second-order Raman scattering and the temperature dependence of the ferroelectric soft mode in ABO_3 perovskites are explained quantitatively in terms of a nonlinear shell model by assuming an anisotropy in the oxygen polarizability. This model yields a new explanation for the origin of ferroelectricity in perovskites.

In 1960 Cochran and Anderson¹ developed the soft mode concept, which explains the ferroelectric phase transition in a great variety of ionic crystals. In this theory a compensation of long- and short-range forces leads to a strongly anharmonic behavior of the ferroelectric soft mode, $\omega_F \equiv \omega_{T_10}(\Gamma)$, whose temperature dependence is approximately described by

$$\omega_F^2 = A(T - T_c). \quad (1)$$

In the last fifteen years, many experimental and theoretical studies have been carried out in order to further clarify the details of the soft mode behavior,² particularly in the ABO_3 perovskites. The explanation of the temperature dependence of the soft mode in terms of anharmonic interactions has been discussed³⁻⁷ and quantitative results have been obtained using an effective quartic potential between the central B ion and its neighboring O ions.^{4,5,7} In order to describe the temperature dependence of ω_F , however, an unrealistic fourth-order parameter had to be used.^{4,7}

In this Letter we show that in ABO_3 perovskites the behavior of the ferroelectric soft mode and related properties may be explained by the strongly anisotropic deformability of the oxygen ion, which also determines the second-order Raman scattering in these crystals.

The following facts led us to focus our attention on the polarizability of the oxygen ion: (a) The only perovskites which are known to show ferroelectric soft modes are the oxidic ones; (b) these are also the only ones which show a strong second-order Raman effect; (c) in simple cubic oxides (such as MgO , etc.), the Raman scattering is dominated by the *intra*-ionic polarizability of the oxygen ion⁸⁻¹⁰; and (d) it is known that the oxygen polarizability depends strongly on its environment in a crystal.¹¹⁻¹³

In order to account for the intra-ionic anisotropy of the oxygen polarizability $\alpha(O^{2-})$, we modify the shell model of Cowley¹⁴ and Stirling¹⁵ by replacing the core-shell force constant by a tensor with two parameters, K_{OA} and K_{OB} (cf. Table I). We denote the corresponding components of the tensor $\alpha(O^{2-})$ in the directions of neighboring A and B ions by α_{OA} and α_{OB} , respectively. Calculations have been performed for $SrTiO_3$ and $KTaO_3$. Both crystals are cubic and show a ferroelectric soft mode, but they differ strongly in the ionic masses and charges. In the case of $KTaO_3$, only the lower phonon branches have been measured by neutron spectroscopy,¹⁶ and the results are therefore less reliable. In order to calculate the second-order Raman spectra, we use a nonlinear extension of $\alpha(O^{2-})$.

TABLE I. Harmonic shell model parameters. The upper values correspond to SrTiO₃, the lower to KTaO₃. The symbols are defined in Ref. 14 and in the text.

A_{OA}	B_{OA}	$e^2/2v$				Z_A	Z_B	e			K_A	e^2/v		
		A_{OB}	B_{OB}	A_{OO}	B_{OO}			Y_A	Y_B	Y_O		K_B	K_{OA}	K_{OB}
26	-4.25	285	-43	1.9	0.74	1.62	3.3	2.3	-1.5	-2.7	57	1446	624	98.97
13	-0.25	340	-62	5.0	0.0	0.95	4.6	4	7	-2.7	1000	525	500	189.95

The two parameters of the quartic intra-ionic Raman polarizability in the isotropic case, H_1 and H_2 ,¹⁷ have to be replaced by four parameters in the present anisotropic case. Corresponding to the second derivatives of $\alpha(O^{2-})$ with respect to displacements in one of the A or B directions, we have nonlinear core-shell coupling parameters $K_{OB,B}$, $K_{OB,A}$, $K_{OA,A}$, and $K_{OA,A'}$. In Fig. 1, the contribution of $K_{OB,B}$ to the second-order Raman spectra is shown for KTaO₃.¹⁸ No improvement is obtained by including the contributions related to $K_{OB,A}$, $K_{OA,A}$, or $K_{OA,A'}$. Considerations of symmetry show that the T_{2g} component of the Raman tensor vanishes identically for the mechanism considered. The agreement between the experimental data and the one-parameter theory, which is based on very restricted experimental phonon data, is remarkable. In SrTiO₃,

the intensity of the high-frequency bands is too weak. In this case we expect that inter-ionic Sr-O polarizabilities contribute to the spectra as in SrO.¹⁰

The softening of ω_F is essentially related to the near instability of the position of the B ion against displacements in the direction of neighboring oxygen ions. Thus, it seems obvious to study the influence of the dominating nonlinear coupling parameter $K_{OB,B}$ on this mode.

For this purpose we use the simplest approximation, calculating the thermal average of the complete quasi-harmonic core-shell B spring of the oxygen ions,

$$K_{OB}(T) = K_{OB} + \frac{1}{2} K_{OB,B} \langle W_B^2 \rangle_T, \quad (2)$$

where $\langle W_B^2 \rangle_T$ is the thermal average of the oxygen shell displacements in the B direction, which is given by

$$\langle W_B^2 \rangle_T = (\hbar/2Nm_0) \sum_{\lambda} [f_{\alpha}^2(O_{\alpha}|\lambda)/\omega_{\lambda}] \coth(\hbar\omega_{\lambda}/2kT). \quad (3)$$

The f 's are shell eigenvectors, $\lambda \equiv (\vec{q}, j)$, and the other quantities are given in a standard notation.¹⁷ O_{α} denotes the oxygen whose neighboring B ions lie in α direction (x , y , or z). The tem-

perature dependence of ω_F is given by

$$\omega_F^2(T) = \omega_0^2 + \frac{1}{2} (K_{OB,B} f_O^2 / M_O) \langle W_B^2 \rangle_T + \text{higher order terms}, \quad (4)$$

where ω_0 is the harmonic frequency, which is imaginary, and f_O is the shell eigenvector of the oxygen whose B neighbors lie in the direction of polarization of the ferroelectric mode. ω_0 and f_O are complicated functions of the harmonic parameters. The higher order terms are smaller than the second term by a factor of 10^{-3} . In Fig. 2 the experimental data for $\omega_F(T)$ in SrTiO₃ and KTaO₃ are compared with the theoretical curves calculated from Eq. (4). The agreement is within the experimental error. The values of $K_{OB,B}$ are obtained by least-square fits, which yield 749 and 500 e^2/va^2 for SrTiO₃ and KTaO₃, respectively, where v means the volume of the elementary cell and a the lattice constant. However, we note that the functional form of the theoretical curves is completely determined by $\langle W_B^2 \rangle_T$. The parameter $K_{OB,B}$ scales this function and contributes to

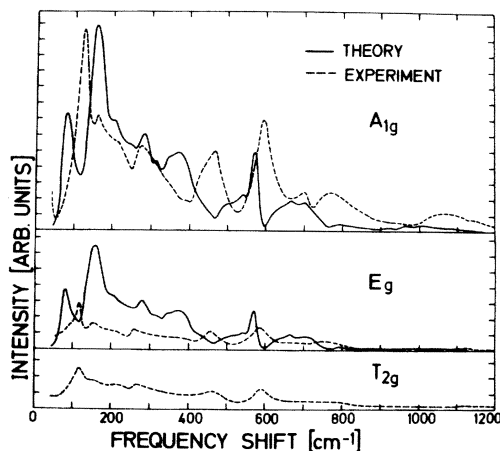


FIG. 1. Second-order Raman spectra of KTaO₃. The intensity scale is the same for the three components.

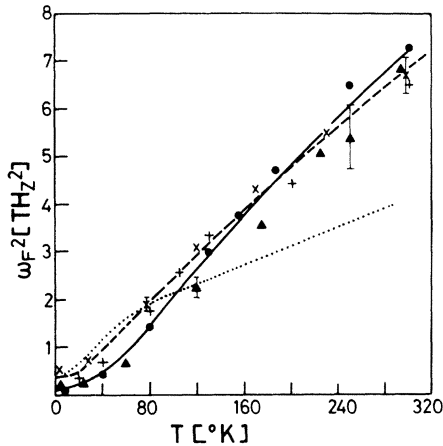


FIG. 2. Temperature dependence of the ferroelectric soft modes. The lines correspond to model calculations: solid line, SrTiO₃; dashed line, KTaO₃; dotted line, KTaO₃ with O isotropically polarizable. Experimental data: SrTiO₃, solid circles (Ref. 19) and solid triangles (Ref. 20); KTaO₃ ×'s (Ref. 21), and +'s (Ref. 19).

the zero temperature value of ω_F^2 . This becomes evident from Fig. 2, which shows a positive value for $\omega_F^2(0)$ although ω_0^2 is negative. The zero point correction includes in a natural way the coupling of the ferroelectric mode to the acoustic modes via $\langle W_B^2 \rangle_T$. We emphasize that the anisotropy of $\alpha(O^{2-})$ in the harmonic model is essential for the curvature of $\omega_F^2(T)$. This can be seen from a calculation for KTaO₃ in which an isotropic polarizability, $K_{OB} = K_{OA}$ is assumed. In this case $K_{OB,B}$ is fitted to the low temperature part of $\omega_F^2(T)$. As shown by the dotted line in Fig. 2, the resulting temperature dependence is much too weak. If, on the other hand, the fit is done in such a way as to describe the mean temperature slope, strong deviations from the experimental data appear at low and high temperatures.

Our model also allows us to understand the stress-induced ferroelectric phase transition in SrTiO₃ and KTaO₃.^{22,23} The lattice constant increases in the plane perpendicular to the uniaxial stress. This results in an increase of the oxygen polarizability, or decrease of $K_{OB,B}$ in this plane. The complete curve for $\omega_F^2(T)$ is therefore shifted to lower frequencies, corresponding to an increase in transition temperature. We believe that in the homologous systems BaTiO₃ and KNbO₃ the ferroelectric phase transition may be explained in a similar way. The correlation between Eqs. (4) and (1) can be seen if we expand the hyperbolic cotangent in Eq. (3). In the "line-

ar" region ($T > 30$ K for KTaO₃ and $T > 60$ K for SrTiO₃) we can write the approximate results

$$A = (kK_{OB,B}f_O^2/2Nm_O^2)\sum_{\lambda}f_{\alpha}^2(O_{\alpha}|\lambda)/\omega_{\lambda}^2, \quad (5)$$

and

$$T_c = -\omega_0^2/A. \quad (6)$$

In contrast to the constant A in Eq. (1), the quantity defined in Eq. (5) is slightly decreasing with increasing temperature due to the renormalization of the $f_{\alpha}(O_{\alpha}|\lambda)$.

A final important point is the consistency of the numerical values $K_{OB,B}$ with the ratio of the second-order Raman and the Rayleigh intensities, which is approximately given by

$$I^{\text{Raman}}/I^{\text{Rayleigh}} = (K_{OB,B}\langle W_B^2 \rangle_T/2K_{OB})^2. \quad (7)$$

For SrTiO₃, Eq. (7) yields a value of 13×10^{-4} . We have measured this quantity and found a lower limit of 8×10^{-4} , which is in sufficient agreement with the theoretical result.

In conclusion, we have shown that the strong Raman scattering and the behavior of the ferroelectric soft mode in oxidic perovskites originate from the unusual anisotropic polarizability of oxygen. This explains why such behavior has not been observed in other perovskites, such as the fluorides; and it helps us to understand the partial success of former calculations with effective oxygen- B -metal potentials. The large anisotropy of the oxygen ion could not be explained by simple considerations including the radii of the A and B ions. Indeed, such a model would lead to a larger polarizability in the A rather than in the B direction. Therefore, we suggest that α_{OB} is enhanced, especially dynamically, by the hybridization of the oxygen p states with the d states of the transition metal ion B . This model is supported by the fact that in other perovskites, such as the aluminates, no ferroelectric soft mode has been observed. The origin of the anisotropy of the oxygen polarizability will be further clarified experimentally and theoretically by investigating perovskites which differ only in the B ion, such as the pairs KTaO₃-KNbO₃ or PbTiO₃-PbZrO₃. Furthermore, the effect of hybridization will be investigated in a microscopic theory. A detailed description of our work will be given elsewhere.

The authors are grateful to Dr. R. Zeyher and Dr. I. R. Gomersall for critical reading of the manuscript.

¹W. Cochran, Adv. Phys. **9**, 387 (1960); P. W. Anderson, in *Fizika Dielektrikov*, edited by G. I. Skamavi

(Akad. Nauk SSSR, Fizicheskii Inst. Lebedeva, Moscow, 1960).

²For recent reviews see J. Scott, *Rev. Mod. Phys.* **46**, 83 (1974); N. S. Gillis, in *Dynamical Properties of Solids*, edited by G. K. Horton and A. A. Maradudin (North-Holland, Amsterdam, 1975), Vol. 2.

³B. D. Silverman and R. I. Joseph, *Phys. Rev.* **129**, 2062 (1963).

⁴R. A. Cowley, *Philos. Mag.* **11**, 673 (1965).

⁵A. Hüller, *Z. Phys.* **220**, 145 (1969).

⁶E. Pytte, *Phys. Rev. B* **9**, 3758 (1972).

⁷A. D. Bruce and R. A. Cowley, *J. Phys. C* **6**, 2422 (1973).

⁸R. Haberkorn, M. Buchanan and H. Bilz, *Solid State Commun.* **12**, 681 (1973).

⁹M. Buchanan, R. Haberkorn, and H. Bilz, *J. Phys. C* **7**, 439 (1974).

¹⁰R. Migoni, K. H. Rieder, K. Fischer, and H. Bilz, to be published.

¹¹J. R. Tessman, A. H. Kahn, and W. Shockley, *Phys. Rev.* **92**, 890 (1953).

¹²E. Paschalis and A. Weiss, *Theor. Chim. Acta* **13**, 381 (1969).

¹³R. Kirsch, A. Gérard, and M. Wautelet, *J. Phys. C*

7, 3633 (1974).

¹⁴R. A. Cowley, *Phys. Rev.* **134**, A981 (1964).

¹⁵W. Stirling, *J. Phys. C* **5**, 2711 (1972).

¹⁶R. Comès and G. Shirane, *Phys. Rev. B* **5**, 1886 (1972).

¹⁷A. D. Bruce and R. Cowley, *J. Phys. C* **5**, 595 (1972).

¹⁸This result is at variance with an earlier discussion (Ref. 10), in which we were misled by the large discrepancies between the neutron data of Stirling (Ref. 15) and of M. Iizumi *et al.*, *J. Phys. C* **6**, 3021 (1973). Dr. Stirling has recently confirmed his earlier results. We are grateful to him for his kind communication. (Refer to W. Stirling and R. Cürrat, to be published).

¹⁹P. A. Fleury and J. M. Worlock, *Phys. Rev.* **174**, 613 (1968).

²⁰Y. Yamada and G. Shirane, *J. Phys. Soc. Jpn.* **26**, 366 (1969).

²¹G. Shirane, R. Nathans, and V. J. Minkiewicz, *Phys. Rev.* **157**, 396 (1967).

²²W. J. Burke and R. J. Pressley, *Solid State Commun.* **9**, 191 (1971).

²³H. Uwe and T. Sakudo, *J. Phys. Soc. Jpn.* **38**, 183 (1975), and *Phys. Rev. B* **13**, 271 (1976).

Intrinsic and Defect-Induced Surface States of Cleaved GaAs(110)*

G. M. Guichar, C. A. Sebenne, and G. A. Garry

Laboratoire de Physique des Solides, associé au Centre National de la Recherche Scientifique, Université Pierre et Marie Curie, 75005 Paris, France

(Received 12 July 1976)

Photoemission-yield-spectroscopy measurements are reported for a set of cleaved *n*-GaAs(110) surfaces, clean or gradually oxygen covered. Depending on the cleavage, the Fermi level at the clean surface is observed at the bulk position or toward midgap. For the first time, the existence of surface states in the gap, close to the conduction band is directly demonstrated when the density of the defect-induced surface states found near the valence-band maximum is small.

During the last few years, there has been an increasing number of investigations, both experimental and theoretical, on electronic properties of semiconductor surfaces. On the whole, general agreement has been found for the electronic and crystallographic surface properties of semiconductors such as silicon and germanium. However, for cleaved (110) surfaces of GaAs, the matter seems to be still controversial, and contradictory results have been reported for the position of the Fermi level at the surface and the existence of surface states in the gap. Dinan, Galbraith, and Fischer¹ reported a large band bending (≈ 0.8 eV) for *n*-type samples and interpreted their results in terms of a band of surface acceptors with its lower edge 0.85 eV below the conduction-band minimum (CBM). In early ultraviolet-photoemission-spectroscopy (UPS) experi-

ments, Eastman and Grobman² found a band of surface states near the valence-band maximum (VBM). Gregory and co-workers^{3,4} repeated these experiments and could not detect any filled states in the band gap, but they claimed that an empty surface-state band "pins" the surface Fermi level at midgap on *n*-type GaAs. It has recently been reported by Eastman and Freeouf⁵ that the filled states in Ref. 2 were not reproducible and that they have detected by photoemission partial-yield measurements a band of unoccupied surface states, the bottom of which would be located about 0.7 eV above the VBM. However, there is a discrepancy between these results and those of Van Laar and Scheer⁶ and, more recently, Huijser and Van Laar⁷ who reported Kelvin measurements on *n*- and *p*-type GaAs (110) surfaces which they interpreted as indicating no Fer-